Gas-Phase NMR Investigation of Structural Exchange in Sulfur Tetrafluoride. Evidence for Nonstatistical Intramolecular Vibrational Redistribution

Cheryl A. Spring and Nancy S. True*

Contribution from the Department of Chemistry, University of California, Davis, California 95616. *Received May 2, 1983*

Abstract: The pressure dependence of axial-equatorial fluorine exchange rates of sulfur tetrafluoride obtained from exchange-broadened gas-phase ^{19}F NMR spectra are compatible with intramolecular vibrational redistribution rates approximately an order of magnitude slower than the statistical limit, indicating that this molecule is not ergodic at ca. 12 kcal/mol. At energies near the pseudorotation barrier, SF_4 has only ~70 vibrational states per cm^{-1}. The temperature dependence of the axial $\rightleftharpoons$ equatorial fluorine exchange rates is consistent with an activation energy for axial-equatorial fluorine exchange of 12.1 (7) kcal/mol. The corresponding previously determined liquid-phase value is 11.2 (1.0) kcal/mol. The higher gas-phase activation energy is compatible with a process occurring via a transition state which is smaller than the equilibrium configuration.

Introduction

This study investigates the gas-phase kinetics of structural exchange in sulfur tetrafluoride (SF_4) and associated intramolecular vibrational redistribution (IVR), intermolecular energy transfer, and solvent effects.

A fundamental question that is still unanswered is under what conditions does statistical IVR occur in molecules.[1-5] It is clearly established that small molecules with low (up to ca. 5 kcal/mol) internal vibrational energy are adequately described by Schrödinger stationary-state models which rigorously exclude any intramolecular vibrational redistribution in the absence of collisions.[6] Conversely, large molecules with internal energies in excess of ca. 40 kcal/mol display statistical IVR.[7] To date, the structure and energy dependence of the transition region between the two extremes is not well characterized.

At present few experimental results sensitive to IVR rates at moderate internal energies are available. Recently, infrared fluorescence measurements from 23 representative molecules varying in size from methane to norbornane demonstrated that a vibrational state density of ca. $10/cm^{-1}$ is necessary for collisionless IVR to occur.[8a] In these experiments one quantum of vibrational energy was initially deposited in a C-H stretching vibration and therefore subsequent fluorescence measurements probed relaxation in molecules with ca. 8.5 kcal/mol of internal energy. These results agree with earlier studies of C_1-C_4 hydrocarbons initially excited in the first C-H overtone vibration (~17 kcal/mol of vibration energy) which reported a critical vibrational-state density of ca. 15 states/cm^{-1} for the onset of collisionless IVR.[8b] Very high resolution vibrational overtone and combination spectra of HCN and its isotopic species, measured between 15 000 and 18 500 cm^{-1} using intracavity photoacoustic spectroscopy, are unperturbed. In this region, classical trajectory calculations yielded power spectra consistent with stochastic IVR.[9] Infrared fluorescence decay studies of oxalyl fluoride (COF-COF) yield intermode vibrational relaxation rates which are extremely rapid and possibly collisionless.[10] The presence of a high vibrational state density associated with the internal torsion possibly allows for rapid vibrational relaxation. Conversely, rigid COF_2 requires approximately 300 collisions to fully equilibrate the vibrational levels. Intramolecular rate processes in highly vibrationally excited benzene, probed through line-shape analyses of C-H vibrational overtone spectra obtained using intracavity dye laser techniques and photoacoustic detection, are rapid but not statistical.[11,12] At the decomposition energy of fluoroalkyl cyclopropanes, ca. 46-47 kcal/mol, vibrational relaxation is found to be statistical, and accordingly the associated decomposition reactions of fluoroalkyl cyclopropanes follow RRKM kinetics.[13] Pressure-dependent rates for the methyl isocyanide isomerization reaction (E_{act}, ca. 37 kcal/mol) are also consistent with RRKM theory.[7]

Noid et al. have reviewed several calculational approaches toward determining the onset of stochastic behavior in molecules.[1] Generally, studies based on classical trajectory approaches are consistent with an onset of stochastic behavior at internal energies between one-third and one-half the molecular dissociation energy.[14-18] Corresponding quantum mechanical studies yield higher results, and the nature of the relation between the quantum mechanical and classical results is not clear at the present time.[19-22]

All these experimental and theoretical studies do, however, indicate that some critical vibrational-state density is essential for rapid intramolecular vibrational redistribution. However, the nature of this dependence and whether other structural features are important are not known. Studies at intermediate energies are useful for further progress in this area. Traditionally, rates of unimolecular conversion in the falloff and second-order regimes have provided direct tests of the rapidity of intramolecular energy flow in critically energized molecules.[7] Since dynamic NMR experiments are sensitive to processes with activation energies ranging from ca. 5 to 20 kcal/mol and the pressure dependence of exchange rates is experimentally obtainable, these studies can provide direct information pertinent to IVR in thermal systems of moderately excited molecules.

Sulfur tetrafluoride is one of the simplest molecules to undergo a structural exchange process which can be conventiently studied by NMR spectroscopy. Most of the extensive existing literature on this system concerns the nature of the fluorine-fluorine ex-

(1) Noid, D. W.; Koszykowski, M. L.; Marcus, R. A. *Annu. Rev. Phys. Chem.* **1981**, *32*, 267-309.
(2) Oref, I.; Rabinovitch, B. S. *Acc. Chem. Res.* **1979**, *12*, 166-175.
(3) Parmenter, C. S. *J. Phys. Chem.* **1982**, *86*, 1735-1750.
(4) Smalley, R. E. *J. Phys. Chem.* **1982**, *86*, 3504-3512.
(5) Stannard, P. R.; Gelbary, W. M. *J. Phys. Chem.* **1981**, *85*, 3592-3599.
(6) Flynn, G. W. *Acc. Chem. Res.* **1981**, *14*, 334-341.
(7) Robinson, P. A.; Holbrook, K. A. "Unimolecular Reactions"; Wiley-Interscience: New York, 1972, and references cited therein.
(8) (a) Stewart, G. M.; McDonald, J. D. *J. Chem. Phys.* **1983**, *78*, 3907-3915. (b) Nesbitt, D. J.; Leone, S. R. *Chem. Phys. Lett.* **1982**, *87*, 123-127.
(9) (a) Lehrman, K. K.; Scherer, G. J.; Klemperer, W. *J. Chem. Phys.* **1982**, *76*, 6441-6442. (b) Lehrman, K. K.; Scherer, G. J.; Klemperer, W. *J. Chem. Phys.* **1982**, *77*, 2853-2861.
(10) Allik, T. H.; Flynn, G. W. *J. Phys. Chem.* **1982**, *86*, 3673-3677.
(11) Bray, R. G.; Berry, M. J. *J. Chem. Phys.* **1979**, *71*, 4909-4922.
(12) Reddy, K. V.; Heller, D. F.; Berry, M. J. *J. Chem. Phys.* **1982**, *76*, 2814-2837.
(13) Meagher, J. F.; Chao, K. J.; Barker, J. R.; Rabinovitch, B. S. *J. Phys. Chem.* **1974**, *78*, 2535-2539.
(14) McDonald, J. D.; Marcus, R. A. *J. Chem. Phys.* **1976**, *65*, 2180-2192.
(15) Wolf, R. J.; Hase, W. L. *J. Chem. Phys.* **1980**, *73*, 3779-3790.
(16) DeLeon, N.; Berne, B. J. *J. Chem. Phys.* **1981**, *75*, 3495-3510.
(17) DeLeon, N.; Berne, B. J. *J. Chem. Phys.* **1982**, *77*, 283-289.
(18) Brummer, P.; Duff, J. W. *J. Chem. Phys.* **1976**, *65*, 3566-3574.
(19) Weissman, Y.; Jortner, J. *J. Chem. Phys.* **1981**, *77*, 1469-1485.
(20) Weissman, Y.; Jortner, J. *J. Chem. Phys.* **1981**, *77*, 1486-1500.
(21) Kay, K. G. *J. Chem. Phys.* **1980**, *72*, 5955-5975.
(22) Stratt, R. M.; Handy, N. C.; Miller, W. H. *J. Chem. Phys.* **1979**, *71*, 3311-3322.

0002-7863/83/1505-7231$01.50/0

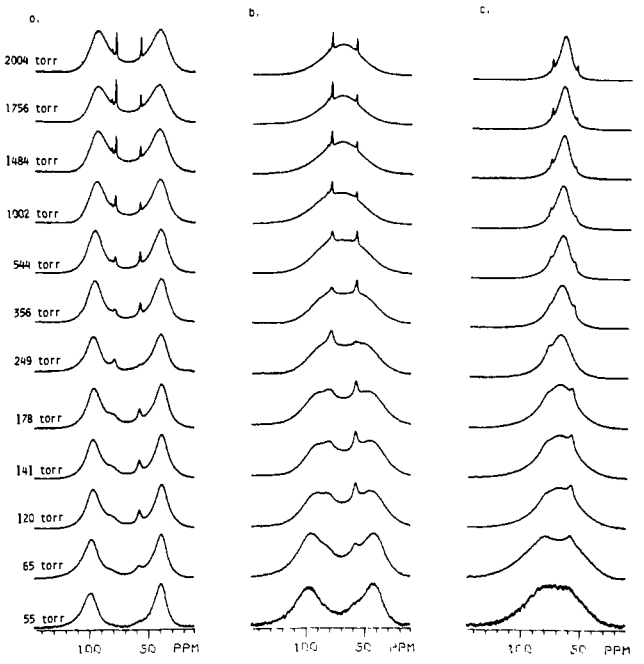

Figure 1. Pressure-dependent exchange-broadened ^{19}F NMR spectra of SF_4 at (a) 308 K, (b) 328 K, and (c) 348 K. Limiting axial and equatorial resonances are at 97.73 and 37.03 ppm, respectively, referenced to $CFCl_3$. Sharp resonances at 56.21 and 77.19 ppm, apparent in the high-pressure samples, are due to SF_6 and SOF_2 impurities, respectively.

change mechanism.[23] Recent studies of very pure liquid samples demonstrate that the temperature-dependent spectral effects observed are attributable to an intramolecular process having the permutational character of a Berry pseudorotation.[24] The liquid-phase activation energy for this process is ca. 11.2 (1.0) kcal/mol.[25] Catalytic amounts of HF can, however, result in faster rates and activation energies ranging from 4 to 5 kcal/mol. This has caused confusion in the early literature.[26] Far-infrared spectral data are consistent with a spectroscopic barrier of 10.2 kcal/mol assuming a C_{4v} transition state.[27] Previous gas-phase NMR studies of SF_4 investigated the temperature dependence of chemical shielding in the fast exchange limit[28] and determined activation parameters for a sample containing 5 atm of gas.[25]

Sulfur tetrafluoride has a low vibrational state density, ca. 70 states per cm^{-1} near the critical energy for axial–equatorial fluorine exchange, and pressure-dependent studies of exchange rates can provide insight into IVR rates in this system. The present study reports temperature- and pressure-dependent axial–equatorial exchange rates in gaseous SF_4, determines the activation energy, and compares details of the falloff region to model calculations assuming statistical IVR. Solvent effects and collision efficiencies associated with this exchange process are also discussed.

Experimental Section

All NMR measurements were made with a Nicolet 200-WB spectrometer with fluorine observation at 188.247 MHz using a 12-mm ^{19}F probe. Samples were contained in 12-mm Pyrex NMR tubes. Spectra were obtained for nonspinning samples and were acquired in an unlocked mode. Acquistion times were typically 22.5 ms per transient, reflecting the rapid relaxation of gaseous ^{19}F nuclei. Typically 600 to 42000 transients were collected at each temperature and their sum was stored in 4K of memory. The resulting spectra as shown in Figure 1 have signal/noise ratios of at least 25/1. Samples were allowed to equilibrate for 5–10 min at each temperature depending on the sample pressure prior to spectral acquistion. The temperature was measured between 173 and 423 K with a copper–constantan thermocouple placed in an empty 12-mm NMR tube and was found to be constant within the active volume of our gas-phase samples. Thermocouple readings were used to calibrate the spectrometer temperature control settings over the experimental temperature range.

Sulfur tetrafluoride was purchased from Matheson Gas Co. and contained approximately 5% SOF_2 impurity and approximately 0.2% SF_6 impurity. Samples were trap-to-trap distilled to remove traces of HF, SiF_4, SF_6, and some SOF_2 using the procedure outlined by Klemperer et al.[24] Between 4 and 17 torr of $CFCl_3$ was added to each sample as a frequency reference. Small amounts of sodium fluoride were also added to act as a HF getter. The sample tubes and the vacuum manifold were flamed out with a torch prior to sample preparation. The line was repeatedly filled with ca. 100 torr of SF_4 for 15-min periods in order to remove any traces of water and HF from the system prior to filling NMR samples. All pressure measurements were made using a Baratron capacitance manometer with a 100-torr head equipped with an analog readout. Sample tubes were attached to the vacuum line with $^1/_8$-in. o.d. capillary tubing. High-pressure samples were prepared by quantitative transfer from calibrated gas bulbs. After filling, the samples were frozen in liquid nitrogen and the tubes were sealed with a torch. Pressures were corrected for the residual volume after sealing. A 2% uncertainty results from this sample sealing technique. All samples were made up immediately prior to use and were kept in liquid nitrogen when not in use. Samples with the compositions listed in Table I were made. Pressures refer to the pressures when the samples were sealed at 298 K.

Rates were calculated with the program DNMR3-IT2 which utilizes a nonlinear least-squares regression analysis to obtain the best fit of the experimental spectrum.[29] Typically 180 experimental points were used in the analysis of each spectrum. The shapes of exchange broadened NMR spectra of SF_4 are dependent on T_2, the effective line-width parameter, the limiting frequency shift between the two magnetically inequivalent sites, spin–spin coupling constants, and the exchange rate. The effective line-width parameter, T_2, was obtained at 213 and 418 K for pressures under 800 torr and at 233–243 and 393–408 K for pressures above 800 torr and was estimated for each sample assuming a linear temperature dependence at each temperature where experimental rate data were obtained. Additional T_1 measurements at pressures above the T_1 minimum, where T_1 and T_2 are equivalent, agree with the T_2 values obtained from direct line-width measurements. All free induction decays were multiplied by an exponential line-broadening factor of ca. 20 Hz to improve the spectral signal/noise, and the resulting contribution to the effective T_2 value was added in for each analyzed spectrum. A limiting chemical shift difference of 60.70 ppm was obtained from spectra acquired at 213 K. This compares with the reported limiting chemical shift of 55.4 ppm obtained in the liquid phase.[30] The smaller limiting shift difference in liquid samples may be due to association in the liquid.[31] Evidence of ^{19}F spin–spin coupling is totally absent in low-temperature gas-phase ^{19}F spectra of SF_4. At 213 K, the full widths at half maximum (fwhm) of the axial and equatorial fluorine resonances are 736 (7) and 556 (7) Hz, respectively, for the 55-torr sample and 326 (5) and 281 (4) Hz, respectively, for the 2004-torr sample. The natural line width of both the axial and equatorial fluorine resonances for all the pressures studied at 213 K exceeds the reported 76.3-Hz value of the axial-equatorial fluorine coupling constant.[31,32] Therefore the molecule was analyzed as an uncoupled AX system. Only rates were varied in the least-squares analysis. Rates obtained from our exchange-broadened spectra have 5–10% uncertainties for spectra within 20 K of the coalescence temperature due to estimated uncertainties in T_2 and uncertainties in the positions of the fluorine resonances and from our spectral signal/noise ratio. The temperature dependence of the rates was used to determine activation energies in the customary way. Results are reported at the 95% confidence level.

Since it was not possible to remove the impurities from our SF_4 samples, additional data were obtained at 308 K for a sample containing 18 torr of SF_6 and 445 torr of SF_4. The exchange rate obtained for this sample agrees with the value interpolated from rate data for a sample pressure of 460 torr.

(23) Jesson, J. P.; Muetterties, E. L. In "Dynamic Nuclear Magnetic Resonance Spectroscopy"; Jackman, L. M.; Cotton, R. A., Eds.; 1974; 253–313.
(24) Klemperer, W. G.; Krieger, J. K.; McCreary, M. D.; Muetterties, E. L.; Traficante, D. D.; Whitesides, G. M. *J. Am. Chem. Soc.* **1975**, *97*, 7023–7030.
(25) Seel, F.; Gombler, W. *J. Fluorine Chem.* **1974**, *4*, 327–331.
(26) Muetterties, E. L.; Phillips, W. D. *J. Chem. Phys.* **1967**, *46*, 2861.
(27) Levin, I. W.; Harris, W. C. *J. Chem. Phys.* **1971**, *55*, 3048–3049.
(28) Jameson, C. J.; Jameson, A. K.; Wille, s. *J. Chem. Phys.* **1981**, *74*, 1613–1617.
(29) Binsch, G.; Klier, D. A. Program No. 356, Quantum Chemistry Program Exchange, Indiana University, Bloomington, IN.
(30) Gibson, J. A.; Ibbott, D. G.; Janzen, A. F. *Can. J. Chem.* **1973**, *51*, 3203–3210.
(31) Bacon, J.; Gillespie, R. J.; Quail, J. W. *Can. J. Chem.* **1963**, *41*, 1016–1018.
(32) Gombler, W.; Seel, F. *J. Fluorine Chem.* **1974**, *4*, 333–339.

Table I. Sulfur Tetrafluoride Exchange Rates (k (s^{-1}) × 10^3). Column Headings Refer to Sample Pressures in torr at 298 K

T (K)	2004	1892	1756	1484	1262	1002	799	796	643	544
296	4.4 (0.6)						5.7 (0.9)		4.7 (0.3)	4.1 (0.4)
300	5.8 (1.2)						5.7 (0.9)		5.5 (0.4)	5.2 (0.5)
304	7.1 (0.8)						7.4 (1.0)		6.8 (0.5)	6.9 (0.6)
308	9.1 (1.3)	10.0 (1.0)	10.9 (1.3)	9.8 (0.8)	9.7 (1.0)	9.1 (0.8)	9.2 (1.2)	8.7 (1.3)	8.5 (0.7)	8.3 (0.7)
312	12.9 (1.8)						11.7 (1.7)		10.2 (0.9)	10.4 (0.9)
316	18.2 (1.9)						14.8 (1.3)		13.1 (1.0)	13.0 (1.4)
320	25.1 (2.4)						18.2 (1.6)		17.2 (1.0)	16.4 (1.4)
322	26.2 (2.4)									
324	26.9 (2.0)						23.3 (2.5)		23.5 (1.8)	22.1 (2.0)
326	32.8 (2.4)									
328	36.9 (1.8)	35.8 (1.4)	35.9 (2.0)	35.5 (2.1)	34.9 (2.0)	32.3 (2.5)	30.0 (1.7)	27.3 (1.1)	29.1 (1.1)	28.6 (1.8)
330	46.1 (3.2)									
332	51.3 (2.7)						38.1 (1.9)		37.1 (3.2)	37.1 (2.5)
336	63.6 (4.4)						46.0 (2.5)		47.9 (2.9)	46.5 (2.9)
340							57.1 (4.3)		60.0 (3.8)	56.9 (4.6)
344							66.6 (2.9)		73.2 (6.0)	74.8 (5.4)
348	130 (11)	97 (11)	110 (8)	106 (11)	101 (10)	90.0 (8.6)	80.4 (4.1)	73.7 (6.0)	105.2 (8.2)	103.4 (7.9)
352										
356										

T (K)	445	356	301	249	204	178	148
296							
300		4.5 (0.3)					
304		5.7 (0.5)			4.9 (0.8)	4.7 (0.7)	4.8 (1.3)
308	7.7 (0.7)	7.4 (0.5)	6.6 (0.9)	6.3 (1.0)	5.6 (0.9)	6.5 (1.0)	5.9 (1.3)
312		9.2 (0.8)			7.6 (1.1)	7.8 (0.6)	7.2 (0.9)
316		10.5 (1.1)			10.4 (1.4)	4.6 (0.8)	8.7 (0.9)
320		13.8 (1.6)			12.2 (1.3)	12.2 (1.2)	11.6 (1.5)
322							
324		19.5 (2.2)			16.7 (1.1)	14.5 (1.2)	15.5 (1.5)
326							
328	24.1 (1.6)	26.2 (2.5)	25.6 (1.7)	24.9 (2.5)	21.6 (2.6)	18.4 (0.9)	20.0 (2.37)
330							
332		30.9 (2.1)			28.7 (2.9)	24.6 (2.3)	26.8 (2.1)
336		39.2 (2.7)			36.1 (3.8)	32.1 (3.6)	32.5 (2.8)
340					41.9 (4.0)	33.7 (3.3)	39.8 (4.0)
344		68.9 (7.5)			47.1 (3.4)	39.0 (3.0)	42.1 (3.6)
348	61.4 (4.2)	90.0 (8.2)	64.6 (6.2)	61.8 (5.8)	55.8 (4.6)	44.9 (2.4)	52.7 (4.1)
352		145.4 (14.5)					
356							

T (K)	141	120	100	80	76.5	65	60	55
296								
300								
304		4.2 (0.5)	3.5 (0.9)		3.1 (0.6)	3.1 (0.5)		2.0 (0.9)
308	5.8 (0.6)	5.5 (4.0)	3.9 (1.2)		4.0 (0.6)	4.0 (0.7)	4.2 (1.7)	2.5 (1.1)
312	7.1 (0.6)	6.6 (0.7)	5.3 (1.3)		4.9 (0.9)	4.9 (1.0)		3.5 (1.4)
316	8.4 (0.8)	8.2 (0.6)	6.7 (1.2)	6.3 (1.1)	6.2 (1.0)	6.2 (0.9)		4.4 (1.7)
320	11.0 (0.9)	9.8 (1.0)	9.1 (1.5)	6.9 (1.7)	8.2 (1.3)	7.4 (1.4)		5.7 (1.9)
322								
324	13.8 (0.9)	13.3 (1.1)	10.7 (2.9)	9.4 (2.8)	10.4 (1.9)	8.9 (1.4)		7.2 (3.1)
326					12.6 (2.6)		10.3 (3.1)	
328	16.7 (1.8)	16.4 (1.0)	13.6 (3.9)	11.1 (2.9)		10.9 (1.5)		8.4 (3.8)
330					15.6 (2.8)	13.4 (1.8)		
332	23.2 (1.8)	21.0 (1.5)	20.0 (3.8)	16.5 (4.1)	19.5 (2.9)	17.3 (3.1)		10.8 (4.3)
336	25.9 (3.3)	22.6 (2.2)	22.0 (4.3)	19.0 (4.5)	23.4 (4.5)	22.0 (2.2)		13.4 (4.6)
340	32.5 (3.6)	30.5 (2.8)			29.8 (4.0)	25.7 (2.0)		17.4 (4.5)
344	38.5 (4.8)	29.7 (3.4)	32.6 (4.5)	28.5 (6.0)	38.0 (8.7)	31.6 (2.6)	28.3 (6.4)	23.6 (5.4)
348	39.7 (5.1)	39.4 (3.6)	39.4 (7.2)	34.1 (6.2)	39.8 (6.3)			
352					48.1 (8.1)			33.5 (7.7)
356								39.4 (13.7)

In order to obtain the temperature dependence of the spin rotation cross sections for use in subsequent kinetic calculations, pressure-dependent T_1 experiments were performed at 423, 253, and 223 K.[33] The time stability of a 141-torr sample was checked by repeating measurements at 308 K after holding the sample at ~425 K for a 2-h period.

Results

Pressure-dependent gas-phase NMR spectra of SF_4 at 308, 328, and 348 K are shown in Figures 1a, 1b, and 1c, respectively. Spectra for the 55-torr sample at 308 K show the axial and equatorial fluorine resonances partially resolved at 97.73 and 37.03 ppm downfield from $CFCl_3$, respectively. Gombler and Seel assign the downfield resonance to the axial fluorines[32] and results of our T_1 relaxation measurements confirm this assignment.[33] The sharp resonances at 56.21 and 77.19 ppm, apparent in the high-pressure samples, are due to SF_6 and SOF_2 impurities which could not be removed. At higher temperatures and pressures, dynamic lineshape effects are apparent. At 308 K, rates for the 55-torr sample are more than a factor of 2 slower than those of the 2004-torr sample. A complete list of experimental exchange rates appears in Table I.

Figure 2 displays the pressure dependence of exchange rates for SF_4 at 328 and 308 K. Both bimolecular and unimolecular kinetic regions are observed. The exchange reaction follows bi-

(33) Spring, C. A.; True, N. S., manuscript in preparation.

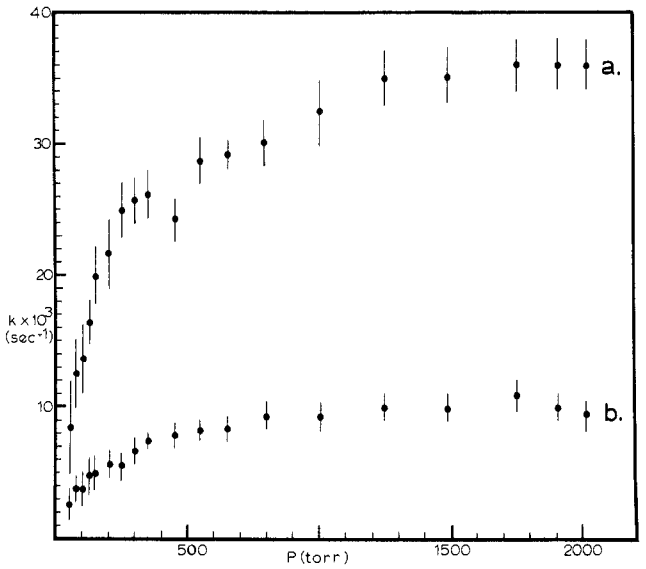

Figure 2. Pressure dependence of axial ⇌ equatorial ^{19}F exchange rates of SF_4 at (a) 328 K and (b) 308 K.

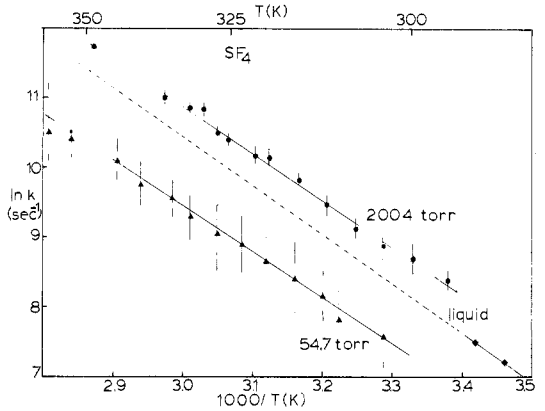

Figure 3. Arrhenius plot for high (2004 torr) and low (55 torr) pressure gas samples of SF_4. The liquid data are from ref 25.

molecular kinetics up to ca. 200 torr at all three temperatures. Above ca. 500 torr, the observed kinetics are unimolecular and rates are independent of pressure within our experimental uncertainties. Based on these results, samples containing 2004 and 55 torr of SF_4 were used to obtain unimolecular and bimolecular activation energies, respectively. For both of these samples, the temperature dependence of the exchange rates appears in Figure 3. The corresponding unimolecular and bimolecular activation energies are 13.6 (7) and 12.5 (4) kcal/mol. Activation energies obtained at intermediate pressures show a 1–2 kcal/mol scatter and a significant difference between a unimolecular and bimolecular activation energy cannot be clearly established. Figure 3 also displays data obtained for liquid SF_4 in a previous study[25] which we have extrapolated into our experimental temperature region. Limiting high-pressure gas-phase rates for SF_4 inversion are significantly slower than rates observed in carefully purified liquid samples. Activation energies for structural exchange in SF_4 are listed in Table II.

Discussion

Gas-phase thermal rate data for SF_4 can be used to probe kinetic questions involving rates of both intra- and intermolecular energy transfer in this small molecule at moderate (ca. 12 kcal/mol) levels of vibrational excitation. Also, direct comparison of gas-phase and liquid-phase data allow the direction and extent of solvent effects to be elucidated. These topics are discussed sequentially below.

For a unimolecular process, the pressure at which the transition between second-order and first-order kinetics occurs is a measure

Table II. Activation Energies for Pseudorotation in Sulfur Tetrafluoride

	E_{act} (kcal/mol)
gas at 2004 torr[a]	13.7 (0.5)
gas at 55 torr[a]	12.5 (0.5)
gas at ca. 3500 torr[b]	11.7 (1.5)
liquid[b]	11.2 (1.0)

[a] This work. [b] Reference 25.

Table III. Normal Mode Assignment of SF_4

species		frequency (cm^{-1})	description[a]
A1	ν_1	891.5	ν sym, SF_2 eq
	ν_2	558.4	ν sym, SF_2 ax.
	ν_3	356[b]	δ sciss SF_2 eq and ax sym comb
	ν_4	228[b]	δ sciss SF_2 eq and ax. asym comb
A2	ν_5	474	SF_2 twist
B1	ν_6	730	ν asym SF_2 ax.
	ν_7	532	SF_2 eq wagging
B2	ν_8	867	ν asym SF_2 eq
	ν_9	350	δ sciss SF_2 ax. out of plane

[a] Reference 37. [b] Pseudorotation modes.

of the rapidity of chemical reaction in critically energized molecules. The falloff curves for SF_4 which are shown in Figure 2 can be characterized by the pressure at which the observed rate has fallen to one-half of its limiting high-pressure value ($P_{1/2}$). At all three temperatures, $P_{1/2}$ is ca. 170 torr, indicating that reaction is occurring in this system on a nanosecond time scale. Using a rotationally inelastic collision diameter of 2.19 obtained from pressure-dependent T_1 measurements, the average lifetime between collisions at 170 torr is 3.8×10^{-9} s at 328 K, and the corresponding rate is 2.6×10^8 s^{-1}. The minimum reaction rate, K_{min}, for critically energized molecules can be obtained from vibrational-state densities. SF_4 has a calculated state density, ρ, of 60/cm^{-1} and ~100/cm^{-1} at energies of 12.7 and 14 kcal/mol with use of spectroscopic data appearing in ref 34 and 35 and a Rabinovitch–Setzer direct count procedure.[34] Minimum rates ($K_{min} = c/\rho$ where c is the speed of light) consistent with these state densities are 5×10^8 and 3×10^8 s^{-1}, respectively, very close to our observed value. In order to determine if we can differentiate between slow and rapid (i.e., statistical) IVR in SF_4, we can compare details of our falloff curves to results of model calculations. Limiting rates, and also rates in the falloff and bimolecular region, were calculated using RRKM theory[34,35] which assumes rapid statistical IVR.

In order to determine if the pseudorotation kinetics of SF_4 can be described by RRKM theory, we can calculate rates within this framework. Assuming the applicability of RRKM theory, one can use the Eyring equation to calculate the ratio of the magnitudes of the partition functions of the transition state to the ground state:

$$\frac{z^{\ddagger}}{z_{eq}} = \frac{Lk_{NMR}h}{\kappa k_B T} \exp(E_0/RT) \qquad (1)$$

where k_{NMR} is the observed exchange rate, $\kappa = {}^1/_2$, and E_0 is the threshold energy. The transition state is assumed to have a square-pyramidal structure,[27] and hence L, the reaction path degeneracy, is 2.[7] Using these values, $z^{\ddagger}/z_{eq}$ is ca. 1 with an uncertainty range of ca. 0.5 to 2.5 assuming threshold energies from 12 to 13 kcal/mol. Rotational constants determined from microwave spectroscopic measurements[36] and vibrational frequencies reported by Christe et al.,[37] shown in Table III, were

(34) Hase, W. L.; Bunker, D. L. Program No. 234, Quantum Chemistry Program Exchange, Indiana University, Bloomington, IN.
(35) Hase, W. L. In Dynamics of Molecular Collisions, Part B., Miller, W. H., Ed.; In "Modern Theoretical Chemistry"; Plenum Press, New York, 1976; pp 121–169.
(36) Tolles, W. M.; Gwinn, W. D. *J. Chem. Phys.*, **1962**, *36*, 1119–1121.
(37) Christe, K. O.; Curtis, E. C.; Schack, C. J.; Cyvin, S. J.; Brunvold, J.; Sawodny, W. *Spectrochim. Acta Part A* **1976**, *32*, 1141–1147.

used to define the equilibrium configuration. For the transition state, the two frequencies corresponding to the pseudorotation, 228 and 356 cm^{-1}, were replaced by a frequency of 182 cm^{-1} which was calculated to yield the observed partition function ratio, z^*/z_{eq} of ~ 1.[35] The ratio of the rotational partition functions was held at 1 and all the other frequencies in the ground and transition state were assumed equivalent. For z^*/z_{eq} ratios of 0.5 and 2.5, which correspond to our uncertainty limits, the corresponding transition state frequencies are 364 and 63 (5) cm^{-1}, respectively. Transition-state sums and vibrational-state densities were evaluated by the direct counting method for these models and were used to calculate the pressure dependence of the falloff.[35] Rates in the falloff and bimolecular region were obtained by solving

$$k_{uni} = \int_0^\infty \int_0^\infty \frac{k_a(E_v^*,E_r^*)P(E_v^*)P(E_r^*)\,dE_v^*dE_r^*}{1 + k_a(E_v^*,E_r^*)/\omega} \qquad (2)$$

$P(E_v^*)$ and $P(E_r^*)$ are the Boltzman distributions, $P(E_v^*) = N(E_v^*)\exp(-E_v^*/kT)/Q_v$, and $P(E_r^*) = N(E_r^*)\exp(-E_r^*/kT)/Q_r$, where $N(E_v^*)$ and $N(E_r^*)$ are the densities of vibrational and rotational quantum states, respectively, and Q_v and Q_r are the molecular vibrational and external rotational partition functions, k_a is the energy-dependent microscopic rate, and ω is the collision frequency.[35] This equation was solved for our system by exact numerical integrations. Spin-rotation cross sections for SF_4 were obtained from T_1 measurements at 223 and 253 K under slow exchange conditions and at 418 K under fast exchange conditions. Corresponding spin-rotation collision diameters are 2.50 (3), 2.44 (2), and 1.87 (4) Å at 223, 253, and 418 K, respectively.[33] A collision diameter of 2.19 Å, interpolated from the temperature dependence of the spin-rotation cross sections, was used in RRKM calculations. The associated experimental uncertainty in this cross section is 0.08 Å. For many systems, spin-rotation cross sections are found to be of similar magnitude to hard-sphere cross sections obtained from transport property measurements.[38] Kinetic cross sections are smaller than hard-sphere cross sections by up to a factor of 100,[7] and 2.19 Å is a maximum reasonable value for this parameter for SF_4. Results of RRKM calculations are shown graphically in Figures 4a, 4b, and 4c. Data and calculations are at 328 K. At other temperatures, the results are qualitatively similar. It is clear that agreement between RRKM calculated rates for pseudorotation in SF_4 and experimental rates is poor for all reasonable models. Figure 4a displays the effect of varying the transition states vibrational partition function, using a model with E_0 of 12.00 and a collision diameter of 2.19 Å. Most notably, all the models predict much faster vibrational relaxation than is observed. $P_{1/2}$ values for the 364-, 182-, and 63-cm^{-1} models and for a 25-cm^{-1} model (corresponding to a z^*/z_{eq} ratio of 5) are 1415, 2270, 5530, and 12,570 torr, respectively, while our observed $P_{1/2}$ value is only 170 torr. For SF_4, the average lifetime between hard-sphere collisions is 3.8×10^{-9} s at 170 torr. Pressures of 1415, 2270, 5530, and 12 570 torr correspond to lifetimes of ca. 2.5×10^{-10}, 1.1×10^{-10}, and 5.3×10^{-11} s, respectively. Using a vibrational frequency of ∞ in the transition state only drops the $P_{1/2}$ value to 940 torr, which is still incompatible with our experimental results. Using other sets of vibrational frequencies which yield the observed partition function ratios has little effect on the pressure dependence of the falloff.

It is informative to consider what changes in the calculational model would have to be made in order to bring the observed and calculated falloff curves into agreement. Reaction rates, according to RRKM theory, are a function of the amount of internal vibrational energy in the molecule and the number of possible ways of distributing it. The effect of varying the internal energy in these calculations is displayed graphically for the 182-cm^{-1} model with a collision diameter of 2.19 Å in Figure 4b. In order to obtain a slower reaction rate and an associated smaller $P_{1/2}$ value in agreement with our experimental results for the falloff curve, it would be necessary in this system to raise the threshold energy

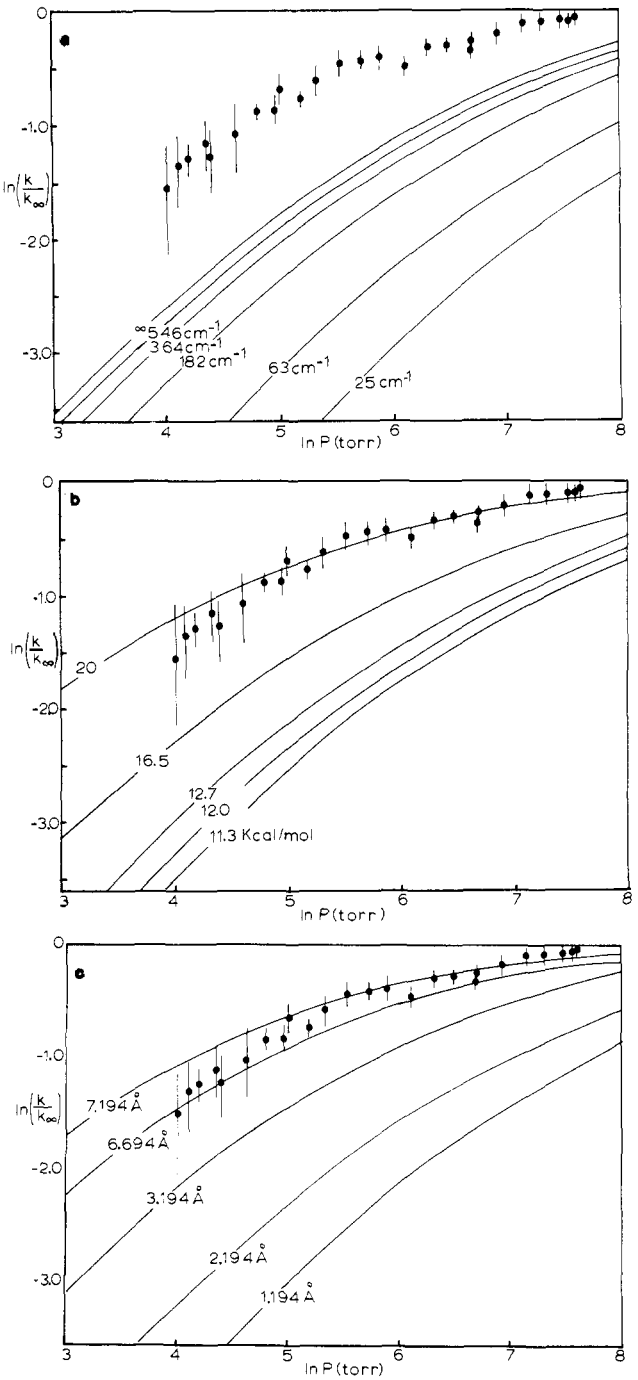

Figure 4. Pressure dependence of axial ⇌ equatorial fluorine exchange rates of SF_4 at 328 K. Experimental points are indicated by circles. Error bars indicate 1 standard deviation in the ratio (k/k_∞): (a) falloff effects due to changing the vibrational frequency in the transition state; (b) variation in falloff using the 182-cm^{-1} model transition state (described in the text) as a function of E_0; (c) variation in falloff using the 182-cm^{-1} model transition state (described in the text) as a function of the collision diameter.

to ca. 20 kcal/mol. The experimental value of this parameter is ca. 12 kcal/mol. Alternately, Figure 4c demonstrates that the calculated curve can be forced to superpose upon the experimental data by allowing the collision diameter to increase by a factor of 3.3. This necessitates using an effective collision diameter of 7.2 Å, or a collisional efficiency parameter of 3.3. In all cases of unimolecular reactions studied to date, collision efficiencies have ranged from 1 to 0.001.[7] Values above 1 are clearly unreasonable.

These calculations demonstrate that SF_4 is not ergodic at ca. 12.5 kcal/mol. RRKM calculations with reasonable input parameters produce reaction rates more than an order of magnitude faster than those experimentally obtained. Fluorescence studies[8a,b]

(38) Wilhelm, E. *J. Chem. Phys.* **1973**, *58*, 3558–3560.

Table IV. Pressure Dependence of Pseudorotation Rates on SF_4 in the Bimolecular Region

T (K)	dk/dP (s^{-1} $torr^{-1}$)[a]	β_c[b,c]
304	15.5 (2.3)	1
308	27.8 (3.5)	1.8 (3)
312	30.7 (2.8)	2.0 (3)
316	32.2 (1.2)	2.1 (3)
320	47.6 (4.2)	3.1 (5)
324	56.4 (5.0)	3.6 (6)
328	79.9 (7.3)	5.1 (4)
332	101.7 (9.2)	6.5 (1.0)
336	135.6 (7.7)	8.7 (1.4)
340	139.8 (7.5)	9.0 (1.4)

[a] Obtained from data at pressures between 55 and 204 torr. [b] $\beta_c = (dk/dP)T/(dk/dP)\ 304K$. [c] Uncertainties are 1 σ.

indicate that SF_4 has a sufficient vibrational-state density for collisionless IVR to occur at ~13 kcal/mol of internal energy. Our results indicate that IVR rates are considerably slower than the statistical limit.

These results may be compared with previously obtained results for cyclohexane inversion in gas mixtures with SF_6.[39] The pressure dependence of ring inversion rates of gaseous cyclohexane is compatible with RRKM calculations using the pseudorotating transition-state model proposed by Pickett and Strauss, indicating statistical IVR in this system. The high-pressure ring inversion activation energy for cyclohexane is 12.5 (5) kcal/mol. At this energy, cyclohexane has a vibrational state density of 1300 states/cm^{-1} which is a factor of 30 greater than that of SF_4 at comparable internal energies. The low vibrational-state density appears to be the critical factor accounting for slower IVR rates of SF_4.

With fluorine observation at 188 MHz, bimolecular rate data for pseudorotation of SF_4 is accessible between ca. 50 and ca. 200 torr. In this pressure region, collisional activation determines the observed pseudorotation rates. The lower and upper pressure limits are due to limitations in signal intensity and the departure from bimolecular kinetics, respectively. Bimolecular rate data were obtained at temperatures between 304 and 340 K for each of ten samples with pressures ranging from 55 to 204 torr (see Table I). The pressure dependence of the rate constants obtained from weighted least-squares regression analysis varies from 15 (2) s^{-1} $torr^{-1}$ at 304 K to 140 (8) s^{-1} $torr^{-1}$ at 340 K and is reported for intermediate temperatures in Table IV. These derivatives were used to determine the temperature dependence of the relative collision efficiencies.[40] Figure 5 displays the natural logarithm of the relative collision efficiency as a function of temperature. The temperature dependence is positive and linear up to 336 K. Collision efficiencies for the activation of the pseudorotation increase exponentially with temperature. A similar dependence has been observed for the syn–anti conformational inversion in methyl nitrite.[41] In that case, the temperature dependence of the collision efficiency obtained over the temperature range 240–280 K was twice as large as that observed over the temperature range 308–340 K for SF_4. The only parameter in these systems that is increasing as an exponential of the temperature

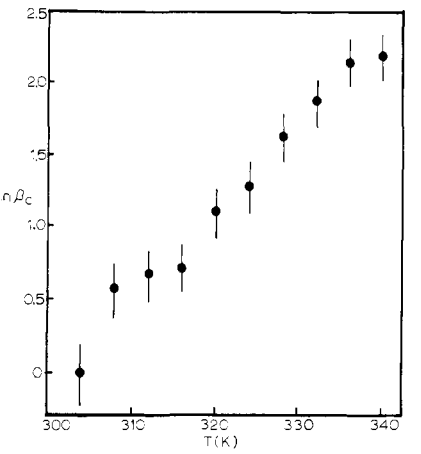

Figure 5. Temperature dependence of SF_4 collisional efficiency.

is the vibrational partition function. The vibrational partition function is ca. 10 for methyl nitrite at 250 K. For SF_4 at 328 K it is ca 4. Internal rotation in methyl nitrite follows RRKM kinetics, whereas pseudorotation in SF_4 does not.

Table II demonstrates that the high-pressure limiting gas-phase activation energy for SF_4 pseudorotation is slightly higher than that observed in carefully purified liquid samples. Two contrasting conclusions are consistent with this observation. It is possible that impurity catalyzed bimolecular exchange is occurring to some extent in the liquid samples. This is unlikely for two reasons. The samples used by Seel and Gombler[25] were very carefully purified. Also, spectral fine structure in the intermediate exchange region obtained by Klemperer et al.[24] is consistent with a process proceeding through a Berry pseudorotation mechanism or one with a similar permutational character. Those experiments were capable of clearly differentiating between pseudorotation and bimolecular exchange mechanism.

An alternate explanation of the higher gas-phase activation energy must consider medium effects. Solvents can perturb the magnitude of kinetic parameters through electrostatic interactions and through internal pressure effects. No significant electrostatic effects would be expected for pure liquid SF_4 since activation energies are not significantly different in various solvents with widely different dielectric constants.[24] Recently, we have observed slower gas-phase rates for cyclohexane ring inversion which correlate with a negative volume of activation for this process.[39] The square-pyrimidal intermediate proposed for the SF_4 pseudorotation process[27] which has the four fluorines in equivalent planar configurations is sterically smaller than the trigonal-bipyramidal equilibrium structure. Accordingly, internal pressure effects in the liquid phase would tend to accelerate rates associated with the exchange process.

Acknowledgment. We are pleased to acknowledge support from the National Science Foundation (Grant CHE82-10844), the Petroleum Research Fund (Grant PRF-13314-G6), and the University of California—Davis Committee on Research. Dr. Gerald Matson of the University of California, Davis NMR Facility, provided valuable help and suggestions. We thank Karl Clark of the University of California, Davis Computer Center, for writing data transfer programs, valuable to our research effort.

Registry No. Sulfur tetrafluoride, 7783-60-0.

(39) (a) Ross, B. D.; True, N. S. *J. Am. Chem. Soc.* **1983**, *105*, 1382–1383. (b) Ross, B. D.; True, N. S. *Ibid.* **1983**, *105*, 4871–4875.
(40) Tardy, D. C.; Rabinovitch, B. S. *Chem. Rev.* **1977**, *77*, 369–408.
(41) Chauvel, J. P., Jr.; True, N. S. *J. Chem. Phys.*, in press.